

Solving the Problem of Electromagnetic Wave Scattering on Small Impedance Particle by Integral Equation Method

Mykhaylo Andriychuk*

Abstract—The problem of electromagnetic (EM) wave scattering on small particles is reduced to solving the Fredholm integral equation of the second kind. Integral representation of solution to the scattering problem leads to necessity to determine some unknown function contained in integrand of this equation. The respective linear algebraic system (LAS) for the components of this unknown vector function is derived and solved by the successive approximation method. The region of convergence of the proposed method is substantiated. The numerical results show rapid convergence of the method in the wide region of the physical and geometrical parameters of problem. Comparison of the obtained results with Mie type and asymptotic solutions demonstrates high degree of accuracy of the proposed method. The numerical results of scattering on particles of several forms and sizes are presented.

1. INTRODUCTION

Investigation of wave scattering on a finite body of an arbitrary shape has continuous history; in this connection, one can note fundamental publications on EM wave scattering [17, 23, 28] and acoustic and light scattering [10, 22, 38], as well the well-known monographs [24, 35], where a variety of methods to their solving were proposed and justified. In the classical work of Mie [21], a rigorous analytical solution for a spherical body was derived. Starting from the middle of last century, the integral equation method (IEM) was applied widely for solving this problem, including acoustic [19] and sound [6] scattering. A variety of numerical methods for solving the light scattering problems were developed in [4]. In works [8, 11, 25, 27], the IEM was developed and applied to the bodies of the non-coordinate form and of different physical properties (impedance, ideally conducting, dielectric bodies). The combination of the IEM with asymptotic techniques [14] and combination of it with iterative methods [13] were applied to solving the scattering problem on conducting bodies. The IEM in conjunction with the Green function method was used in [18, 20, 39] and for solving the diffraction problem on perfectly conducting scatterers. The review of progress, advantages, existing problem and difficulties of the IEM were summarized in [40]. In book [28], the problems related to the specific performances of scattering by small bodies of an arbitrary shape were discussed. The specific methods and algorithms were developed in [16] for solving EM wave diffraction by finite plane array of small bodies.

In conjunction with widely using PC technique and development of computational methods, such numerical method as the method of moment, finite element method, and projective methods were used successfully for solving the specific scattering problems [36, 37, 43].

Despite the presence of such a large number of publications on this topic and diversity of methods to solve related problems, development of methods for solving the scattering problem for the case of a body of an arbitrary shape with specific physical conditions is important. This is because of using the scattering theory in the diverse application areas, such as medical imaging and testing [3], geophysical

Received 2 December 2017, Accepted 14 February 2018, Scheduled 6 March 2018

* Corresponding author: Mykhaylo I. Andriychuk (andr@iapmm.lviv.ua).

The author is with the Pidstryhach Institute for Applied Problems of Mechanics and Mathematics, NASU, Ukraine.

exploration [5], non-destructive testing [9], THz technology [7], moving the antenna technique to new perspective frequency bands [26].

In this paper, we consider the application of the IEM for solving the scattering problem of EM field on an impedance body of an arbitrary shape. The obtained solution will be compared with the previously obtained asymptotic solution and known Mie solution from [2] to determine accuracy of the approach developed here and to define limits of application of these methods. The application of previously developed asymptotic approach of Ramm [30] and proposed method will be used in the future to improve the procedure of creating medium with a given refraction coefficient [1] and permeability [33] by embedding into medium a large number of small particles.

Because of high intrinsic interest for wave scattering by one small impedance particle, the developed approach allows one to generalize it to the case of many particles and to obtain some physically interesting conclusions about changes of material properties of the medium in which many small particles are embedded [31, 32]. These results were presented firstly in paper [29], and they were used for developing a method for creating materials with a desired refraction coefficient by embedding many small impedance particles into a given medium for scalar wave scattering [1], as well as for electromagnetic wave scattering [31]. In contrast to above papers, where the explicit expression of solution to the diffraction problem was obtained, we deal here with another method of solving the scattering problem. The paper discusses the possibility to solve the formulated scattering problem using the solution of obtained Fredholm integral equation of the second kind. The problems, related to investigation of the successive approximation method for LAS, corresponding to this equation, are discussed.

The impedance boundary conditions widely applicable in physics and do not require that the body is small or large. One can pass to the limit in the equation for the effective field [30] in the medium, obtained by embedding many small impedance particles into a given medium. This leads to a need for numerical calculations showing the possibility to use the developed asymptotic theory in the wide range of parameters, such as radius a of the particle, its boundary impedance ζ , distance d between neighboring particles, and wavelength. The numerical results obtained on the basis of the solution to Fredholm integral equation will allow to testify that the asymptotic theory developed in the papers mentioned above is rigorous, and its application to creating media with desired refraction coefficient or permeability is physically defensible.

2. STATEMENT OF PROBLEM

The EM field scattered by a limited particle with smooth boundary S satisfies

$$\nabla \times E = i\omega\mu_0 H, \quad \nabla \times H = -i\omega\varepsilon_0 E \quad \text{in } D' = \mathbb{R}^3 \setminus D, \quad (1)$$

here D is the particle region. The outside medium is described by constant permittivity $\varepsilon_0 > 0$ and constant permeability $\mu_0 > 0$, and ω is the frequency. The impedance boundary conditions have the form

$$[N, [E, N]] = \zeta [H, N] \quad \text{on } S, \quad (2)$$

where ζ is the surface impedance of S , N the outside normal on S , and radiation conditions:

$$E = E_0 + E_s, \quad H = H_0 + H_s, \quad (3)$$

where E_0, H_0 are the components of incident field, and E_s, H_s are the components of scattered field.

In Equation (2) $[E, N] = E \times N$ is a cross product of two vectors.

Equation (1) and boundary conditions in Eq. (2) can be written as:

$$\nabla \times \nabla \times E = k^2 E \quad \text{in } D', \quad H = \frac{\nabla \times E}{i\omega\mu_0}, \quad (4)$$

$$[N, [E, N]] = \frac{\zeta}{i\omega\mu_0} [\nabla \times E, N] \quad \text{on } S, \quad (5)$$

where k is the wavenumber, $k = \omega(\varepsilon_0\mu_0)^{1/2}$, and smallness of a particle means that $ka \ll 1$, where a is the effective radius of scattering.

Hence, the problem can be reduced to determination of one vector E . After its determination, H components are determined by the second formula of Eq. (4).

3. METHOD OF SOLUTION

The vector E is sought in the form [31]

$$E = E_0 + \nabla \times \int_S g(x, t) J(t) dt, \quad g(x, t) = \frac{e^{ik|x-t|}}{4\pi|x-t|}, \tag{6}$$

where $J(t)$ is an unknown function which will be determined below, and $g(x, t)$ is Green function of free space.

In order to obtain the integral equation for function $J(t)$, we substitute the first expression of Eq. (6) into boundary conditions in Eq. (5). Using the know formula [31]

$$\left[N, \nabla \times \int_S g(x, t) J(t) dt \right]_{\mp} = \int_S [N, [\nabla_x g(x, t) J(t)]] dt \pm \frac{J(t)}{2}, \tag{7}$$

where by \mp are marked limit values at passing variable x to boundary S of the domain D outside and inside, and $\nabla_x g(x, t)$ is the derivative of Green function with respect to variable x . We obtain in the general operator form

$$J = AJ + f. \tag{8}$$

Eq. (8) is Fredholm integral equation of the second kind.

Action of operator A and function f are defined as

$$AJ = -2[N, BJ], \quad f = 2[f_e, N]. \tag{9}$$

Operator B acts in such a way

$$B[J(S)] = \left[\int_S [N, [\nabla_x g(x, t), J(t)]] dt, N \right] + \zeta i \omega \varepsilon_0 \left[\int_S g(x, t) J(t) dt, N \right], \tag{10}$$

and function f_e is presented in the form

$$f_e(S) = [N, [E_0(S), N]] - \frac{\xi}{i\omega\mu_0} [\nabla \times E_0(S), N]. \tag{11}$$

Operator A is linear and compact in the space $C(S)$. Therefore, Eq. (8) is of Fredholm type, and it is solvable for any right part $f \in T$ if the homogeneous equation, corresponding to Eq. (8), has only trivial solution $J = 0$. T is a set of all tangential to S continuous vector fields such that $\text{Div} E^t = 0$, where Div is the surface divergence, and E^t is the tangential component of E . The fact that Eq. (8) is solvable verifies

Lemma 3.1 *Assume that $J \in T$, $J \in C(S)$, and $J = AJ$, then $J = 0$.*

One can find the lemma proof in [31].

The cross product in Eqs. (9), (10), and (11) mismatches the components of function J ; this yields the use of the method of successive approximations while passing from Eq. (8) to the respective LAS (see, for example, Eq. (26) below).

4. DETERMINATION OF THE MATRIX COEFFICIENTS OF INTEGRAL EQUATION FOR VECTOR J

In the matrix form Eq. (8) looks like as follows

$$\begin{pmatrix} J_x \\ J_y \\ J_z \end{pmatrix} = \begin{pmatrix} A_{xx} & A_{xy} & A_{xz} \\ A_{yx} & A_{yy} & A_{yz} \\ A_{zx} & A_{zy} & A_{zz} \end{pmatrix} \begin{pmatrix} J_x \\ J_y \\ J_z \end{pmatrix} + \begin{pmatrix} f_x \\ f_y \\ f_z \end{pmatrix}. \tag{12}$$

The right parts of Eq. (12) are expressed by the next formulas

$$f_x = [E_{0y} \cos \theta - E_{0z} \sin \theta \sin \varphi] - \frac{\zeta}{i\omega\mu_0} \left[\left(\frac{\partial E_{0z}}{\partial y} - \frac{\partial E_{0y}}{\partial z} \right) (-\cos^2 \theta - \sin^2 \theta \sin^2 \varphi) + \left(\frac{\partial E_{0y}}{\partial x} - \frac{\partial E_{0x}}{\partial y} \right) \sin \theta \cos \theta \cos \varphi + \left(\frac{\partial E_{0x}}{\partial z} - \frac{\partial E_{0z}}{\partial x} \right) \sin^2 \theta \sin \varphi \cos \varphi \right], \quad (13)$$

$$f_y = [E_{0z} \sin \theta \cos \varphi - E_{0x} \cos \theta] - \frac{\zeta}{i\omega\mu_0} \left[\left(\frac{\partial E_{0x}}{\partial z} - \frac{\partial E_{0z}}{\partial x} \right) (-\sin^2 \theta \cos^2 \varphi - \cos^2 \theta) + \left(\frac{\partial E_{0z}}{\partial y} - \frac{\partial E_{0y}}{\partial z} \right) \sin^2 \theta \sin \varphi \cos \varphi + \left(\frac{\partial E_{0y}}{\partial x} - \frac{\partial E_{0x}}{\partial y} \right) \sin \theta \cos \theta \sin \varphi \right], \quad (14)$$

$$f_z = [E_{0x} \sin \theta \sin \varphi - E_{0y} \sin \theta \cos \varphi] - \frac{\zeta}{i\omega\mu_0} \left[\left(\frac{\partial E_{0y}}{\partial x} - \frac{\partial E_{0x}}{\partial y} \right) (\sin^2 \theta \sin^2 \varphi - \sin^2 \theta \cos^2 \varphi) + \left(\frac{\partial E_{0x}}{\partial z} - \frac{\partial E_{0z}}{\partial x} \right) \sin \theta \cos \theta \sin \varphi + \left(\frac{\partial E_{0z}}{\partial y} - \frac{\partial E_{0y}}{\partial z} \right) \cos \theta \sin \theta \cos \varphi \right]. \quad (15)$$

The components of operator A are determined by

$$A_{xx} = 2 \int_S \left(\frac{\partial g(x, y, z, t')}{\partial y} \sin \theta' \sin \varphi' + \frac{\partial g(x, y, z, t')}{\partial z} \cos \theta' \right) dt' + 2i\zeta\omega\mu_0 \int_S g(x, y, z, t') dt' (-\sin^2 \theta \sin^2 \varphi - \cos^2 \theta), \quad (16)$$

$$A_{xy} = -2 \int_S \frac{\partial g(x, y, z, t')}{\partial x} \sin \theta' \sin \varphi' dt' + 2i\zeta\omega\mu_0 \int_S g(x, y, z, t') dt' \cdot \sin^2 \theta \sin \varphi \cos \varphi, \quad (17)$$

$$A_{xz} = -2 \int_S \frac{\partial g(x, y, z, t')}{\partial x} \cos \theta' dt' + 2i\zeta\omega\mu_0 \int_S g(x, y, z, t') dt' \cdot \sin \theta \cos \theta \cos \varphi, \quad (18)$$

$$A_{yx} = -2 \int_S \frac{\partial g(x, y, z, t')}{\partial y} \sin \theta' \cos \varphi' dt' + 2i\zeta\omega\mu_0 \int_S g(x, y, z, t') dt' \cdot \sin^2 \theta \sin \varphi \cos \varphi, \quad (19)$$

$$A_{yy} = 2 \int_S \left(\frac{\partial g(x, y, z, t')}{\partial z} \cos \theta' + \frac{\partial g(x, y, z, t')}{\partial x} \sin \theta' \cos \varphi' \right) dt' + 2i\zeta\omega\mu_0 \int_S g(x, y, z, t') dt' (-\cos^2 \theta - \sin^2 \theta \cos^2 \varphi), \quad (20)$$

$$A_{yz} = -2 \int_S \frac{\partial g(x, y, z, t')}{\partial y} \cos \theta' dt' + 2i\zeta\omega\mu_0 \int_S g(x, y, z, t') dt' \cdot \sin \theta \cos \theta \sin \varphi, \quad (21)$$

$$A_{zx} = -2 \int_S \frac{\partial g(x, y, z, t')}{\partial z} \sin \theta' \cos \varphi' dt' + 2i\zeta\omega\mu_0 \int_S g(x, y, z, t') dt' \cdot \sin \theta \cos \theta \cos \varphi, \quad (22)$$

$$A_{zy} = -2 \int_S \frac{\partial g(x, y, z, t')}{\partial z} \sin \theta' \sin \varphi' dt' + 2i\zeta\omega\mu_0 \int_S g(x, y, z, t') dt' \cdot \sin \theta \cos \theta \sin \varphi, \quad (23)$$

$$A_{zz} = 2 \int_S \left(\frac{\partial g(x, y, z, t')}{\partial x} \sin \theta' \cos \varphi' + \frac{\partial g(x, y, z, t')}{\partial y} \sin \theta' \sin \varphi' \right) dt' + 2i\zeta\omega\mu_0 \int_S g(x, y, z, t') dt' \cdot \sin^2 \theta. \quad (24)$$

In Equations (16)–(24), variable t' corresponds to the integration point in S with coordinates r', θ', φ' (x', y', z'), and r, θ, φ (x, y, z) are the coordinates of observation point outside S .

Using discretization of Eq. (12), we pass to the respective LAS for determination of J_x, J_y , and J_z components. This LAS for component J_x has the form

$$\tilde{J}_x = \tilde{A}_{xx}\tilde{J}_x + \tilde{A}_{xy}\tilde{J}_y + \tilde{A}_{xz}J_z + \tilde{f}_x, \tag{25}$$

or

$$(I - \tilde{A}_{xx})\tilde{J}_x = \tilde{A}_{xy}\tilde{J}_y + \tilde{A}_{xz}\tilde{J}_z + \tilde{f}_x, \tag{26}$$

where I is the unit matrix, and mark “tilde” indicates the discretized form of operator A components, and functions J and f elements. The formulas for determination of \tilde{J}_y and \tilde{J}_z components are similar to Eq. (26).

It follows from Eq. (26) that for determination of component \tilde{J}_x it is necessary to have values of the rest components \tilde{J}_y and \tilde{J}_z . In this connection, we will use the method of successive approximations for search of \tilde{J} components similar to [13]. In the first stage, we prescribe \tilde{J}_{y0} and \tilde{J}_{z0} ; having these two values, we determine \tilde{J}_{x1} . In the next stage, we determine \tilde{J}_{y1} by \tilde{J}_{x1} and \tilde{J}_{z0} . In the third stage, we determine \tilde{J}_{z1} , using found \tilde{J}_{x1} and \tilde{J}_{y1} .

In accordance with necessary condition of convergence [12], the iterative process for Eq. (26) converges if $\|A\| < 1$. The norm of operator A is understood here as the norm of respective kernel. This leads to a condition on the parameters a, ζ , and ω . This condition can be formulated as

Theorem 4.1 *Let the components of operator A be determined by Equations (16)–(24), and $ka \ll 1$, then the iterative process for solving the integral Fredholm Eq. (8) converges if the condition*

$$12\pi a \zeta \omega \mu_0 < 1 \tag{27}$$

is fulfilled.

Note: Formula (27) is obtained from the necessary condition of convergence of the iterative process to solve system (12). One can obtain more exact estimation while investigating the properties of respective Fredholm operator A in Eq. (8). Such an investigation needs separate attention. The numerical calculations show that the developed algorithm has a smart property: nevertheless there is non-convergence in the first iterations; it becomes the convergence in the next iterations (see, for example, Fig. 4).

5. NUMERICAL RESULTS

The numerical algorithms for solving the diffraction problem in Eqs. (1)–(3) need accurately taking into account of requirements related to convergence of the proposed iterative procedure for determination of the $J(t)$ components by the proposed iterative procedure (see [13]). The numerical results show that domain of convergence for this procedure is wide enough. The characteristic of convergence is investigated for J_x, J_y, J_z components for various values of radius a of particle. The rest parameters of problem are as follows: $\varepsilon_0 = 8.85 \times 10^{-12}$ F/m, $\mu_0 = 4\pi \times 10^{-7}$ H/m, $\omega = 229.86$ GHz ($k = 0.1 \text{ m}^{-1}$), $\zeta = 500$. The values of E components are determined by the explicit formula (6) as soon as the components of J are determined.

5.1. Convergence of Iterative Procedure

In Figs. 1–3, the characteristic problems of iterative process for small values of radius a are presented. One can see that iterative process converges very rapidly. The relative error of solution is determined as degree of accuracy. This error is determined as

$$\text{RE} = \frac{|V_{n+1} - V_n|}{|V_{n+1}|}, \tag{28}$$

where V_n, V_{n+1} are values of the respective components in n th and $n + 1$ th iterations, $V = \{J_x, J_y, J_z\}$. At $a = 1.0$, the relative error for J_x component (see Fig. 1) decreases from 4.28% in the first iteration

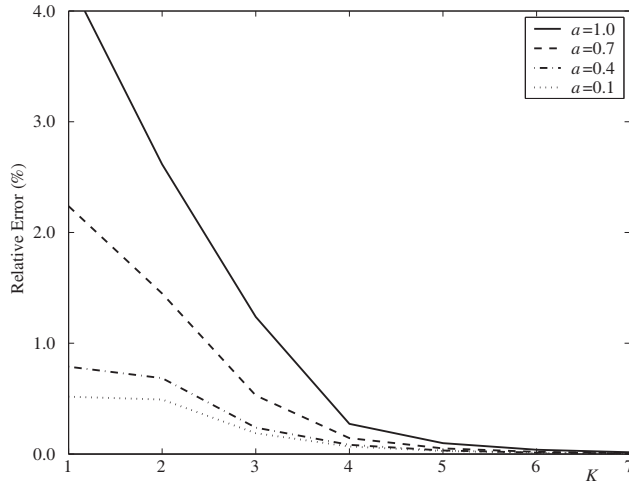


Figure 1. The relative error of J_x component versus number K of iteration.

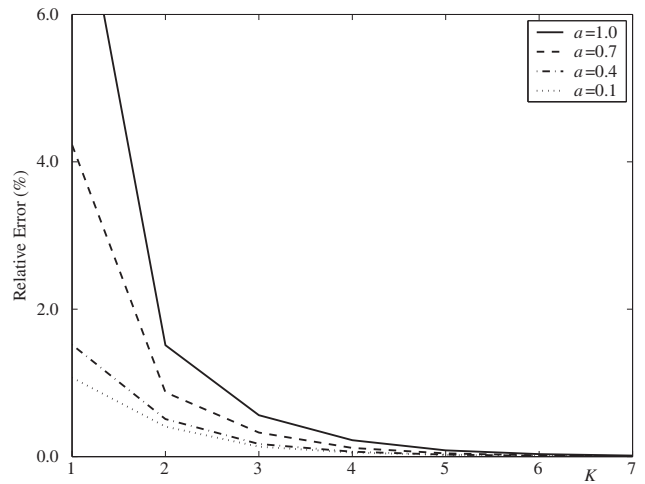


Figure 2. The relative error of J_y component versus number K of iteration.

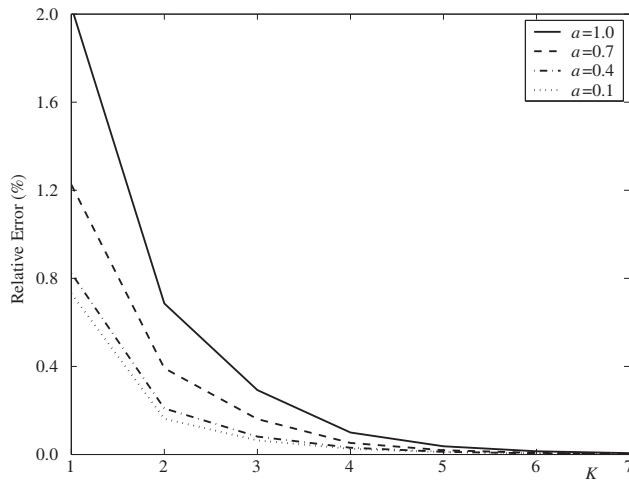


Figure 3. The relative error of J_z component versus number K of iteration.

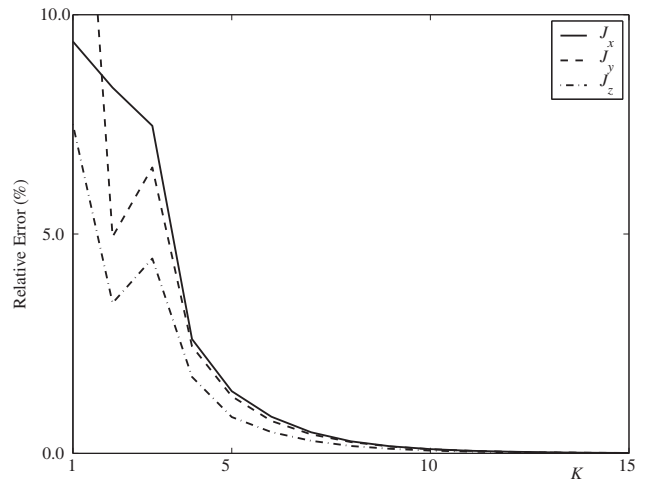


Figure 4. The relative error of J components versus number K of iteration, $a = 5.0$.

to 0.015% in the seventh iteration. This error diminishes if a decreases. So, at $a = 0.1$, the values of relative error are equal to 0.52% and 0.004%, respectively. The respective values of the relative error for J_y component are equal to 8.32% and 0.013% for $a = 1.0$, and 1.07% and 0.004% for $a = 0.1$ (Fig. 2). These values for J_z are equal to 2.03% and 0.006% for $a = 1.0$, and 0.78% and 0.002% for $a = 0.1$ (Fig. 3). Summarizing these results, one can conclude that exactness of the obtained solutions does not exceed several thousandths of percent; therefore, the values of respective E components will be calculated with guaranteed high accuracy.

In order to determine the region of the applicability of the proposed method of successive approximation, we carry out calculations in wide region of parameter a . It is found that with growth of a , the iterative procedure becomes somewhat unstable, and it becomes divergent at $a > 10.0$. This is explained by the fact that the condition in Eq. (27) does not hold at the given ω and ζ .

In Fig. 4, the behavior of convergence is shown at $a = 5.0$. One can see that the convergence for J_y and J_z component is non-monotone. Moreover, the values of relative error are greater than that for small values of a (in the first stage, they are equal to 9.39%, 18.51%, and 7.49% for J_x , J_y and J_z components, respectively). The number of necessary iterations to achieve the same degree of accuracy

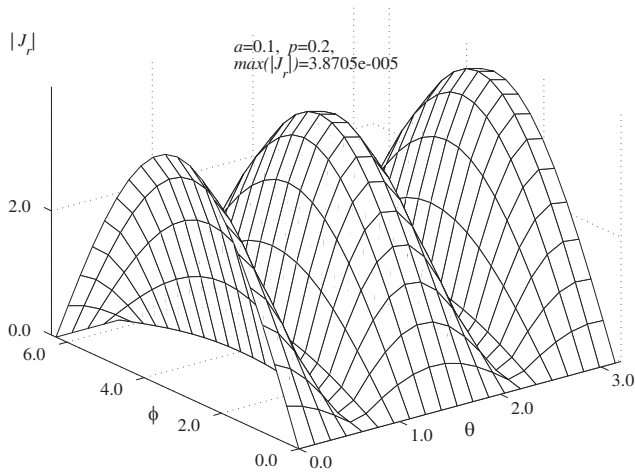


Figure 5. Amplitude of E_r component of the scattered field, $a = 0.1$.

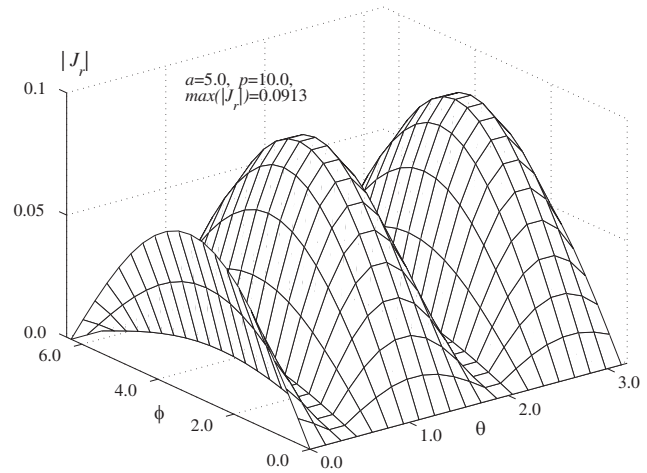


Figure 6. Amplitude of E_r component of the scattered field, $a = 5.0$.

as for small a grows twice. So the relative error equal to thousandths of percent is achieved on 15 iteration, and it is equal to 0.008%, 0.007%, and 0.005% for J_x , J_y and J_z components, respectively.

After determination of the area of convergence of the problem's parameters, one can deal with solving the diffraction problem. The first step consists of solving Eq. (8) by means of passing to LAS corresponding to Eq. (12). Let us consider the case of plane wave $E_0 = \beta e^{ik\alpha \cdot x}$; β is constant vector; α is unit vector, and $\alpha \cdot \beta = 0$. If the components of vector-function J are determined, the values of vector E are determined explicitly by formula (6). For the considered case, vector E has only x -component, and $E_y \equiv E_z \equiv 0$. In practice, the spherical components of electromagnetic field are of much interest to researchers. In this connection, we pass to the spherical components of field using known formulas (see, for example, [15]). In Fig. 5, the amplitude of E_r component is shown for $a = 0.1$, and the rest of parameters are the same as in the previous example. The field components are calculated at the distance $p = 2a$ from the particle center.

The electrical size of a particle at such a is small: in our case $k = 0.1$, therefore total $ka = 0.01$ that corresponds to very small diameter of scattering, and amplitude of scattered field is fifth order lower than the amplitude of incident field that is equal to 1.0 in our case of plane wave. The maximal value of E_r component is equal to 3.87×10^{-5} ; the amplitude diminishes if p grows. In the case that a grows, the form of scattered field changes slightly, but the amplitude increases on several orders. For example, this amplitude is equal to 0.0913 at $a = 5.0$. (see Fig. 6).

5.2. Comparison with Mie Type and Asymptotic Solutions

In order to establish the accuracy of EM field components received by solving LAS for J components and next determining them by formula (6), we compare the received results with Mie type solution received in [2]. Mie type solution is considered here as benchmark one. In Fig. 7, the relative error of our solution is demonstrated for different values of impedance ζ . One can see that relative error grows slightly as ζ increases, but it does not exceed $3 \times 10^{-2}\%$ for the considered values of a . In fact, the relative errors are very close for E_x , E_y , and E_x components; therefore, it is shown for component E_x only. So, at $\zeta = 2000$, this error is equal to $3.1 \times 10^{-5}\%$ at $a = 0.01$, and it grows to $2.7 \times 10^{-2}\%$ at $a = 0.05$. The relative error diminishes if ζ decreases, equals $2.75 \times 10^{-2}\%$ at $\zeta = 2000$, and equals $0.75 \times 10^{-2}\%$ at $\zeta = 500$ for $a = 0.05$.

The numerical calculations carried out for the values of a in the limits from 1.0 to 10.0 for different ζ show that relative error increases not more than one order. This testifies that the accuracy of our solution is very high, and it is comparable to the accuracy of Mie type solution. In this connection, we can consider our new solution as the benchmark one comparing it with the asymptotic solution obtained in [2]. In Fig. 8, the relative error of the asymptotic solution is shown for the same values of parameters

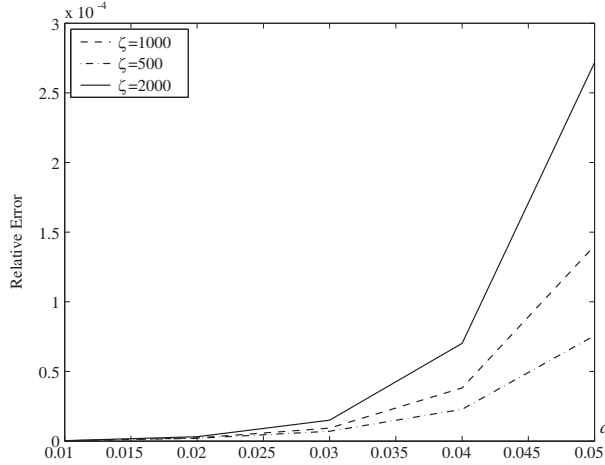


Figure 7. Relative error of new solution for E_x component.

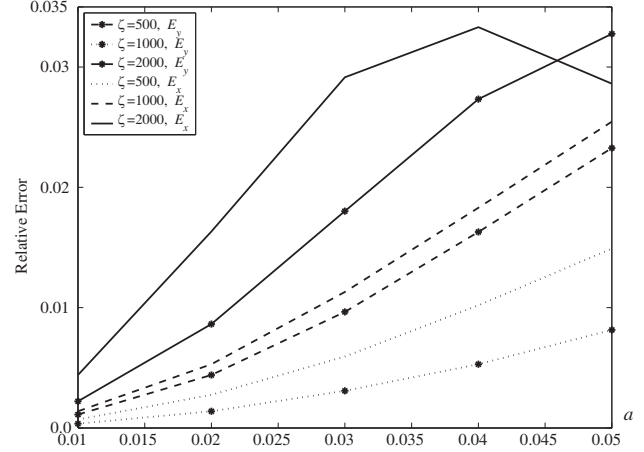


Figure 8. The relative error of asymptotic solution [2].

a and ζ for E_x and E_y components. The maximal value of relative error is attained for E_x component at $\zeta = 2000$ in the point $a = 0.04$, and it is equal to 3.3%. The minimal value of error is equal to 0.43%, and it is attained at $a = 0.01$. The relative errors for E_y and E_z components practically coincide for this case.

The obtained results show that the relative error of asymptotic solution is worse than the relative error in the previous example. In this connection, we compare our new solution with the solution obtained in [34], which is determined by the specified asymptotic formula. This formula contains an additional term taking into account the smallness of a of the particle radius. It is found that the relative error of this specified asymptotic solution is much better than that for the regular asymptotic solution.

In Fig. 9, the relative error of solution obtained in [34] is shown for E_x and E_y components. As in the previous example, our new solution is considered as benchmark one. The plots demonstrate that relative error for this case is much less than in the previous one, and it is close to the relative error of Mie solution. In total, this error is worse on $0.5 \times 10^{-2}\%$ than that for Mie solution. For this case we observe different relative errors for E_x and E_y components only at $\zeta = 2000$. The maximal error is attained for E_x component at $a = 0.05$, and it is equal to $3.9 \times 10^{-2}\%$. The maximal error is attained for E_y component at $a = 0.05$, and it is equal to $4.6 \times 10^{-4}\%$. The relative errors for E_x and E_y components at $\zeta = 500$ and $\zeta = 1000$ practically coincide, and this error for E_z component coincides with relative error for E_y component for all considered ζ . The above results confirm that considering the additional term in the specified asymptotic solution (see [34]) has sense even at large values of a .

Of course, the proposed method cannot rival those proposed in [34] on the required computing time. The calculation of vector E values is carried out by the explicit formulas (3.3) and (3.4) there. Here, we should calculate E by formula (6) that implies solving integral equation (8) for vector J . The main disadvantage is that the elements of matrix A and right part f are respective integrals, and for their calculation we need a lot of time. For example, in [34] one needs about 0.5 sec (taking into account calculation of some preliminary parameters) for calculation E value on PC with CPU 2.4 GHz for the particle with radius $a = 0.01$ cm, $k = 1.0$ cm $^{-1}$, at $\zeta = 500.0$; the calculation by the proposed method needs 1 min, 23.6 sec. However, the first advantage of the last method is that it is applicable to a large set of a values.

The second advantage of method is that it can be applied successfully in the range of small wave lengths, because the respective algorithm is sensitive for product a and k only. For small a and $\lambda(k = 2\pi/\lambda)$ values, ka remains in the limits $1.0 \times 10^{-3} - 1.0$ (nanometer size of particle and micrometer length of wave, for example) that permits to have a good performance of algorithm in the range mentioned above. The numerical calculations show that the amplitude of scattered field diminishes by the respective law if the radius a of particle decreases.

The numerical results, related to calculations with smaller values of ζ parameter, show that relative error can be reduced more than one order. In Fig. 10, the relative error is shown at $\zeta = 20, 50, 80$. One

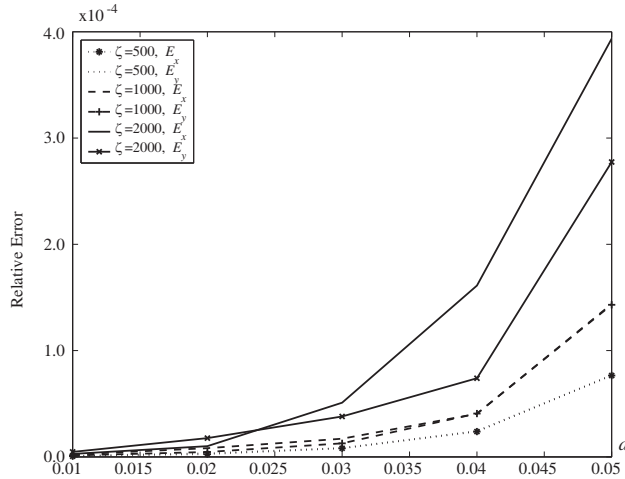


Figure 9. The relative error of specified asymptotic solution [34].

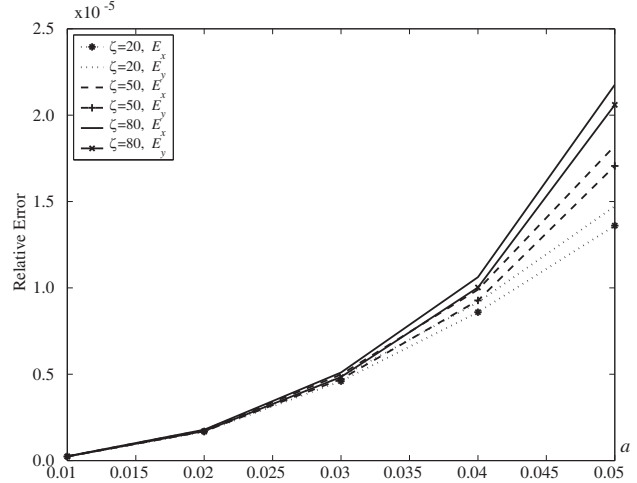


Figure 10. The relative error of specified asymptotic solution [34] for small values of ζ .

can see that the maximal value of relative error is attained for E_x component at $\zeta = 80$, and it is equal to $2.2 \times 10^{-3}\%$. The value of relative error for all components at $a = 0.01$ coincides for all considered ζ , and it is equal about to $2.5 \times 10^{-5}\%$.

Summarizing the presented results, we conclude that the new solution, obtained by solving the Fredholm integral equation with next application of formula (6) is exact enough in the wide range of parameters a and ζ . The relative error in comparison with the Mie type solution does not exceed $3.0 \times 10^{-2}\%$, and relative error of specified asymptotic solution is slightly worse: it does not exceed $4.0 \times 10^{-2}\%$.

5.3. Case of the Ellipsoid Particle

The results, considered in the two previous subsections, concern the case of spherical particle. If we wish to solve the problem for the particle with another geometry, we should take into account the change of the particle form. For example, in the process of numerical solving Fredholm Eq. (8) and LAS respective to it, we should use the actual representation of the element of surface area. So if we pass from investigation of spherical particle to particle in the ellipsoid form, we should change the element of spherical area $dt = a^2 \sin \theta d\varphi d\theta$ by

$$dt = \sqrt{b^2c^2 \cos^4 \theta \cos^2 \varphi + ac \cos^4 \theta \sin^2 \varphi + a^2b^2 \sin^2 \theta \cos^2 \theta} d\varphi d\theta, \tag{29}$$

and to take into account that derivative respectively to r coordinate is not equal to zero on the surface of ellipsoid, in contrast to a spherical particle. The numerical results show that properties of convergence of the method of successive approximations are similar to the case of a spherical particle; this method converges very rapidly for the case that the semiaxes of ellipsoid do not differ in the limits of 20%. If this difference grows, the convergence becomes slowly, and we need twice of the number of iterations to achieve the same accuracy as for spherical particle if $b, c \geq 3a$, where a is the value of semiaxis along x coordinate, b the value of semiaxis along y coordinate, and c the value of semiaxis along z coordinate. The amplitude form of the scattered field does not differ considerably if the semiaxes a, b, c of ellipsoid vary in the limits of 10%.

The numerical results show that amplitude of the scattered field of ellipsoid particle increases more quickly than amplitude of the scattered field of spherical particle while value of semiaxis a grows, and the values b and c remain the same; $k = 0.05 \text{ m}^{-1}$. In Fig. 11 and Fig. 12, the comparative results related to change of the amplitude of E_r component are shown for two cases. In the first case (Fig. 11), the value of semiaxis $b = 3a$ and the value of semiaxis $c = a$. In the second case (Fig. 12), $b = 3a$ and $c = 3a$. The biggest growth of amplitude is observed at $\zeta = 500$. One can see that for this ζ values of the two amplitudes are almost the same at small values of a , and the amplitude increases almost twice

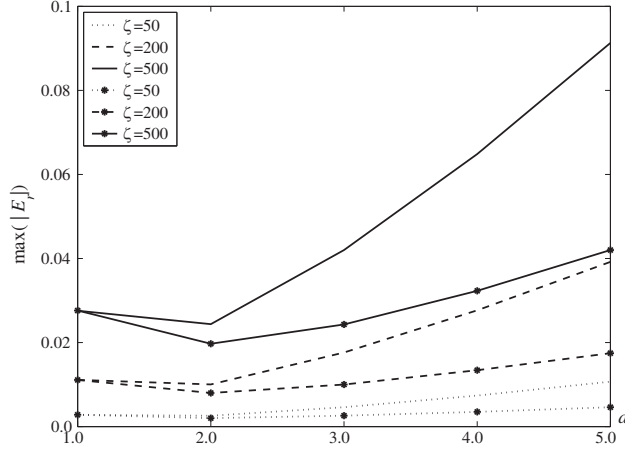


Figure 11. Maximal amplitude of E_r component at semiaxes $b = 3a$, $c = a$.

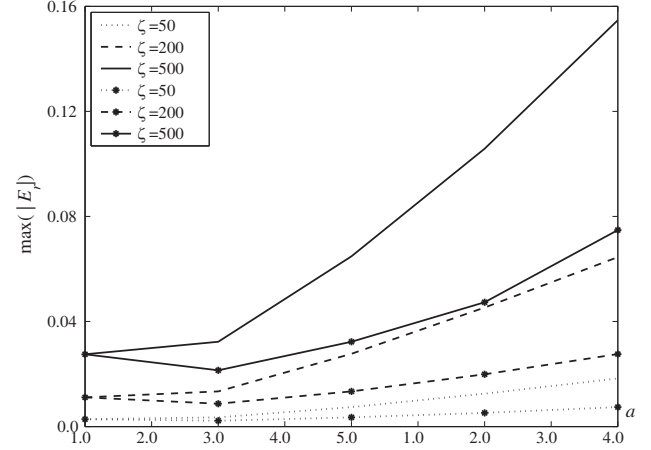


Figure 12. Maximal amplitude of E_r component at semiaxes $b = 3a$, $c = 3a$.

for the second case at $a = 5.0$. The difference of two amplitudes is the biggest at $a = 5.0$, and it is equal to 0.063. Increase of amplitude at smaller ζ is not so great. For comparison, the growth of amplitude for the case of spherical particle with the same a is shown by lines marked with asterisk.

The numerical calculations show that the amplitude of scattered field components for the ellipsoid particle tends to the respective amplitude for the spherical particle, if the values of semiaxes b and c tend to a . This fact confirms the correctness and accuracy of the elaborated method for the case of the ellipsoid particle. The method is generalized for the case of a particle of an arbitrary shape. The main difficulty for such generalization is to elaborate the numerical algorithm for replacement of the analytical representation of the element of area by its numerical analog.

Among a variety of publications, devoted to application of integral equation method to solve EM and acoustic wave scattering problems, one should note the approach proposed in the Chapter “Integral Equation Method for Three-Dimensional Bodies” from book [24], which is closest to our consideration. In [42], the uniform surface integral equation method is applied to the investigation of EM wave scattering by objects with mixed boundary conditions. The obtained set of integral equations is converted to respective LAS using the Galerkin’s technique. The structure of the obtained matrix is similar to the structure of matrix in Eq. (12). Similar to our procedure, the obtained solution is compared with a known Mie type solution for sphere in the near and far zones. The exactness of both the approaches is comparable. The disadvantage of method [42] is that the number of basic functions for sphere with $kr = 1.0$ and respective discretization needs more than 960 unknowns (this is order of respective LAS). In our case, the order of matrices in Eqs. (25), (26) at such kr is about 200.

The numerical procedure to solve the respective LAS in [41] needs calculation of double series (corresponding to space discretization) that yields in matrices of order 1068 at $r = 0.5$ m. The method proposed in [44] is more powerful, but it is applicable to scatterers of rectangular form only. In conclusion, one can substantiate that our method is exact, effective, and it can be applied successfully to solve scattering problems in a wide range of particle’s size and frequency band.

6. CONCLUSIONS

The analytical-numerical method for solving the electromagnetic wave scattering on an impedance particle of an arbitrary shape is elaborated and tested. The integral equation with respect to an unknown function in the representation of solution is derived. The LAS, corresponding to this equation, is solved effectively by the method of successive approximations. It is shown numerically that the region of convergence of the proposed method is wide enough. The physical characteristics of scattering are investigated for the particles with several forms and different sizes. The approach can be generalized for the case of many particles, and it can be used for solving the problems of creating the media with various electromagnetic properties by embedding a big number of small particles in the initial medium.

ACKNOWLEDGMENT

Author thanks Prof. Alexander G. Ramm, Kansas State University, USA, for creative discussions related to the topic under investigation.

REFERENCES

1. Andriychuk, M. I. and A. G. Ramm, "Scattering by many small particles and creating materials with a desired refraction coefficient," *Intern. Journ. of Computing Science and Mathematics*, Vol. 3, No. 1/2, 102–121, 2010.
2. Andriychuk, M. I., S. W. Indratno, and A. G. Ramm, "Electromagnetic wave scattering by a small impedance particle: Theory and modeling," *Optics Communications*, Vol. 285, 1684–1691, 2012.
3. Attaran, A., W. B. Handler, K. Wawrzyn, R. S. Menon, and B. A. Chronik, "Reliable RF B/E-field probes for time-domain monitoring of EM exposure during medical device testing," *IEEE Trans. Antennas Propagat.*, Vol. 65, No. 9, 4815–4823, 2017.
4. Barber, P. W. and S. C. Hill, *Light Scattering by Particles: Computational Methods*, World Scientific, Singapore, 1990.
5. Chen, Y., Y. Ge, G. B. M. Heuvelink, R. An, and Y. Chen, "Object-based superresolution land-cover mapping from remotely sensed imagery," *IEEE Transactions on Geoscience and Remote Sensing*, Vol. 56, No. 1, 328–340, 2018.
6. Faran, J. J., "Sound scattering by solid cylinders and spheres," *J. Acoust. Soc. Amer.*, Vol. 23, No. 4, 405–418, July 1951.
7. Gensheimer, P. D., C. K. Walker, R. W. Ziolkowski, and C. D. D'Aubigny, "Full-scale three-dimensional electromagnetic simulations of a terahertz folded-waveguide traveling-wave tube using ICEPIC," *IEEE Transactions on Terahertz Science and Technology*, Vol. 2, No. 2, 222–230, 2012.
8. Glisson, A. W., "Electromagnetic scattering by arbitrarily shaped surfaces with impedance boundary conditions," *Radio Sci.*, Vol. 27, No. 6, 935–943, November 1992.
9. Helander, J., A. Ericsson, M. Gustafsson, T. Martin, D. Shöberg, and C. Larsson, "Compressive sensing techniques for mm-wave nondestructive testing of composite panels," *IEEE Trans. Antennas Propagat.*, Vol. 65, No. 10, 5523–5531, 2017.
10. Van De Hulst, H. G., *Light Scattering by Small Particles*, Dover, New York, 1981.
11. Ishimaru, A., *Electromagnetic Wave Propagation, Radiation and Scattering*, Englewood Cliffs, Prentice-Hall, NJ, 1991.
12. Kantorovich, L. V. and V. I. Krylov, *Approximate Methods of Higher Analysis*, Noordhoff, Groningen, 1958.
13. Kaye, M., P. K. Murthy, and G. A. Thiele, "An iterative method for solving scattering problems," *IEEE Trans. Antennas Propagat.*, Vol. 33, No. 11, 1272–1279, November 1985.
14. Ko, W. L. and R. Mittra, "A new approach based on a combination of integral equation and asymptotic techniques for solving electromagnetic scattering problems," *IEEE Trans. Antennas Propagat.*, Vol. 25, No. 2, 187–197, March 1977.
15. Korn, G. A. and T. M. Korn, *Mathematical Handbook for Scientists and Engineers*, McGraw-Hill Book Company, 1968.
16. Kyurkchan, A. G. and S. A. Manenkov, "Solving the problem of electromagnetic wave diffraction at a finite plane grating with small elements," *Journal of Quantitative Spectroscopy and Radiative Transfer*, Vol. 180, 92–100, 2016.
17. Landau, L., E. Lifschitz, and L. Pitaevsky, *Electromagnetism of Continuous Medium*, Pergamon Press, Oxford, 1984.
18. Lu, K.-Y., S.-C. Tuan, H.-T. Chou, and H.-H. Chou, "Analytical analysis of electromagnetic transient scattering from perfectly conducting ellipsoidal surfaces illuminated by a plane wave," *Proc. of IEEE International Symposium on Antennas and Propagation (APS-URSI)*, 2523–2526, 2011.

19. Mason, W. P. and R. N. Thurston, "Physical acoustics principles and methods," *Academic*, Vol. XV, 191–202, New York, 1981.
20. Medgyesi-Mitschang, L. N. and J. M. Putman, "Integral equation formulations for imperfectly conducting scatterers," *IEEE Trans. Antennas Propagat.*, Vol. 33, No. 2, 206–214, February 1985.
21. Mie, G., "Beiträge zur Optik trüber Medien, speciell kolloidaler Metallösungen," *Annalen der Physik*, Vol. 330, No. 3, 377–445, 1908.
22. Mishchenko, M. I., L. D. Travis, and A. A. Lacis, *Scattering, Absorption and Emission of Light by Small Particles*, Cambridge University Press, 2002.
23. Müller, C., *Foundations of the Mathematical Theory of Electromagnetic Waves*, Springer-Verlag, Berlin, 1969.
24. Peterson, A. F., S. L. Ray, and R. Mittra, *Computational Methods for Electromagnetics*, 1st Edition, Wiley IEEE Press, 1977.
25. Poggio, A. J. and E. K. Miller, "Integral equation solutions of three dimensional scattering problems," *Computer Techniques for Electromagnetics*, R. Mittra, ed., Chap. 4, Pergamon, Oxford, 1973.
26. Rao, S., "Innovative antenna front ends from L-band to Ka-band," *IEEE Antennas & Propagation Magazine*, Vol. 59, No. 5, 116–129, October 2017.
27. Rao, S. M., D. R. Wilton, and A. W. Glisson, "Electromagnetic scattering by surfaces of arbitrary shape," *IEEE Trans. Antennas Propagat.*, Vol. 30, No. 3, 409–418, May 1982.
28. Ramm, A. G., *Wave Scattering by Small Bodies of Arbitrary Shapes*, World Scientific, Singapore, 2005.
29. Ramm, A. G., "Many-body wave scattering by small bodies and applications," *J. Math. Phys.*, Vol. 48, No. 10, 103511, 2007.
30. Ramm, A. G., "Wave scattering by many small particles embedded in a medium," *Phys. Lett. A*, Vol. 372/17, 3064–3070, 2008.
31. Ramm, A. G., "Electromagnetic wave scattering by many small bodies and creating materials with a desired refraction coefficient," *Progress In Electromagnetics Research M*, Vol. 13, 203–215, 2010.
32. Ramm, A. G., "Scattering by many small inhomogeneities and applications," *Topics in Chaotic Systems, Selected Papers from Chaos 2010 International Conference*, C. Skiadas, I. Dimotikalis, C. Skiadas, ed., 41–52, World Sci. Publishing, 2011.
33. Ramm, A. G. and M. I. Andriychuk, "Application of the asymptotic solution to EM field scattering problem for creation of media with prescribed permeability," *J. Appl. Math. Comput.*, Vol. 45, No. 1, 461–85, 2014.
34. Ramm, A. G. and M. I. Andriychuk, "Calculation of electromagnetic wave scattering by a small impedance particle of an arbitrary shape," *Mathematical Modeling of Natural Phenomena*, Vol. 9, No. 5, 254–269, 2014.
35. Rylander, T., A. Bondeson, and P. Ingelström, *Computational Electromagnetics*, 2nd Edition, Springer, 2012.
36. Sheng, X.-Q., J.-M. Jin, J. Song, C.-C. Lu, and W. C. Chew, "On the formulation of hybrid finite-element and boundary-integral methods for 3D scattering," *IEEE Trans. Antennas Propagat.*, Vol. 46, No. 3, 303–311, March 1998.
37. Soudais, P., "Computation of the electromagnetic scattering from complex 3D objects by a hybrid FEM/BEM method," *Journal of Electromagnetic Waves and Applications*, Vol. 9, No. 7, 871–886, July 1995.
38. Ufimtsev, P. Y., *Axially Symmetric Scattering of Acoustic Waves at Bodies of Revolution (Fundamentals of the Physical Theory of Diffraction)*, Wiley-IEEE Press, 2014.
39. Vesnik, M. V., "Analytical solution for electromagnetic diffraction on 2-D perfectly conducting scatterers of arbitrary shape," *IEEE Trans. Antennas Propagat.*, Vol. 49, No. 12, 1638–1644, December 2001.
40. Wilton, D. R., "Review of current status and trends in the use of integral equations in computational electromagnetics," *Electromagnetics*, Vol. 12, 287–341, 1992.

41. Yang, C. X. and M. S. Tong, "Time-domain analysis of transient electromagnetic scattering from dielectric objects based on electric field integral equations," *IEEE Trans. Antennas Propagat.*, Vol. 65, No. 2, 966–971, 2017.
42. Ylä-Oijala, P., S. P. Kiminki, H. Walln, and A. Sihvola, "Uniform surface integral equation formulation for mixed impedance boundary conditions," *IEEE Trans. Antennas Propagat.*, Vol. 63, No. 12, 5718–5726, 2015.
43. Yuan, X. C., "Three-dimensional electromagnetic scattering from inhomogeneous objects by the hybrid moment and finite element method," *IEEE Trans. Microwave Theory Tech.*, Vol. 38, No. 8, 1053–1058, August 1990.
44. Zhong, Y., M. Lambert, D. Lesselier, and X. Chen, "A new integral equation method to solve highly nonlinear inverse scattering problems," *IEEE Trans. Antennas Propagat.*, Vol. 64, No. 5, 1788–1799, 2016.